

Spring 5-1-2019

Seeing Eye to Eye: A Machine Learning Approach to Automated Saccade Analysis

Maigh Attre
maigh.attre@uconn.edu

Follow this and additional works at: https://opencommons.uconn.edu/srhonors_theses

 Part of the [Artificial Intelligence and Robotics Commons](#), [Bioelectrical and Neuroengineering Commons](#), [Bioimaging and Biomedical Optics Commons](#), [Biological and Chemical Physics Commons](#), [Biomedical Devices and Instrumentation Commons](#), [Diagnosis Commons](#), [Disease Modeling Commons](#), [Equipment and Supplies Commons](#), [Eye Diseases Commons](#), [Graphics and Human Computer Interfaces Commons](#), [International Public Health Commons](#), [Investigative Techniques Commons](#), [Medical Biomathematics and Biometrics Commons](#), [Medical Neurobiology Commons](#), [Musculoskeletal, Neural, and Ocular Physiology Commons](#), [Nervous System Commons](#), [Nervous System Diseases Commons](#), [Neurology Commons](#), [OS and Networks Commons](#), [Other Analytical, Diagnostic and Therapeutic Techniques and Equipment Commons](#), [Other Biomedical Engineering and Bioengineering Commons](#), [Programming Languages and Compilers Commons](#), [Systems and Integrative Engineering Commons](#), and the [Vision Science Commons](#)

Recommended Citation

Attre, Maigh, "Seeing Eye to Eye: A Machine Learning Approach to Automated Saccade Analysis" (2019). *Honors Scholar Theses*. 613.
https://opencommons.uconn.edu/srhonors_theses/613

Seeing Eye to Eye: A Machine Learning Approach to Automated Saccade Analysis

Maigh S. Attre

B. S.

Department of Biomedical Engineering

University of Connecticut, 2019

Honors Thesis Advisor/Honors Advisor: Patrick Kumavor, PhD.

TABLE OF CONTENTS

SECTION	PAGE NUMBER
<i>Abstract</i>	3
<i>Existing Problem and Background</i>	4
<i>Neurological Considerations</i>	4
<i>Optical Considerations</i>	13
<i>Methods, Design, and Experimental</i>	33
<i>Procedure</i>	
<i>Alternative Designs</i>	36
<i>Final Design</i>	45
<i>Results</i>	51
<i>Conclusion and Future Work</i>	60
<i>Acknowledgements</i>	62
<i>References</i>	62
<i>Appendix</i>	67

ABSTRACT:

Abnormal ocular motility is a common manifestation of many underlying pathologies particularly those that are neurological. Dynamics of saccades, when the eye rapidly changes its point of fixation, have been characterized for many neurological disorders including concussions, traumatic brain injuries (TBI), and Parkinson's disease [5, 24, 26, 22]. However, widespread saccade analysis for diagnostic and research purposes requires the recognition of certain eye movement parameters. Key information such as velocity and duration must be determined from data based on a wide set of patients' characteristics that may range in eye shapes and iris, hair and skin pigmentation [36]. Previous work on saccade analysis has primarily been based on presetting patient information such as location of markers (e.g. pupil, iris, caruncle) before and after a saccade. In this paper, a machine learning approach is applied to determine a saccade's dynamics by eye structure identification of static images before and after a saccade. Several machine learning and alternative methods are considered for the identification of the pupil and a static component of the eye such as the caruncle. These include circle detection via the Hough Transform. The incorporation of these approaches aims to reduce computational load, increase broader patient detection, and improve compatibility with various device interfaces. In this report, these tools are explored by applying them to smartphone-captured images of the eye after a saccade is induced simultaneously using the smartphone device.

EXISTING PROBLEM AND BACKGROUND

INTRODUCTION TO NEUROLOGICAL DISORDERS

Neurological disorders are pathologies of the nervous system. This includes over 600 different diseases [16, 31] that can affect the brain, spinal cord, and/or nerves of the system. Their effects can range from affecting basic bodily functions such as breathing and swallowing to more nuanced neurological functions such as learning and memory. The root cause of these diseases varies greatly as does their presentation and comorbidities. Some disorders may be due almost solely to genetic factors like Huntington's disease and muscular dystrophy [16]. The causative issue may be due to events during the developmental stage of the embryo such as spina bifida. Others may be degenerative and cause nerve cells to deteriorate in function and/or die; some common examples of this include Parkinson's disease and Alzheimer's disease. There are disorders that arise from vascular disease especially based on its locational proximity to the brain like stroke. Spinal cord and brain injuries can also lead to further neurological disorders such as concussions. There are seizure disorders like epilepsy. There are neurological cancers and infections as well like brain tumors and meningitis respectively. [16, 31]

CURRENT DIAGNOSTIC PROCEDURES FOR NEUROLOGICAL DISORDERS AND THEIR PEARLS AND PITFALLS

Current diagnostic tests and procedures also can vary based on the type of neurological disorders. These diagnostic tools are also emerging. As the National Institute of Neurological Disorders and Stroke describes, "...[a] century ago, the only way to make a positive diagnosis for many neurological disorders was by performing an autopsy after a patient had died. [19]" However there has been rapid modernization of this field; there are newer techniques now that push to bring as much anatomical and functional information to healthcare providers while minimizing the risk to patients.

There are many common screening tests. One pathway is to complete laboratory screening tests of bodily fluids like urine and blood which can be used diagnostically and also to monitor disease progression as well as response to certain medication. Another pathway is to use genetic testing. This may be in combination with the first method. For example, Huntington's disease can be diagnosed from genetic testing of the DNA from a patient's extracted white blood cells. There are other techniques that are more invasive such as amniocentesis which requires a surgical procedure to test amniotic fluid. For more specific disease diagnostics and for older patient populations, there may be a need for a neurological examination. This is often done by a specialized healthcare practitioner and in a specialized setting such as a doctor's office. There may be reflex testing using flashlights and reflex hammers to check overall neurological function. However, for in depth diagnostics, there may be more involved testing for this as well which may involve psychological evaluation and invasive tools like needles [19].

Of the tools that may be used during a neurological exam, imaging is likely to be used as a first-line tool especially for adults. Many diagnostic techniques deal with the comprehensive visualization of the nervous system. These techniques often require intricate protocols and need to be run in special settings. The operators of the experimental imaging machinery also may need specialized knowledge to operate as do the healthcare providers that interpret the imaging results for each modality. The time required for these can range but can be up to several hours to process and may require patient preparation beforehand. For example, x-rays are common first-line tools but often have too low resolution for more intricate damage and still have the issues of requiring specialized machinery, settings, and personnel. To increase contrast, low-dose radiation may be administered. This may not work for certain populations such as geriatric and pediatric patients [19, 21].

After obtaining patient history, a physical exam, x-rays of the patient's chest and skull, as well as a neurological exam, more specific diagnostic tools may be used as baseline data collection of the patient is finally complete. This may involve diagnostic nuclear medicine imaging such as positron emission tomography and single photon emission computed tomography scans which may be run alongside other more traditional anatomical imaging techniques such as magnetic resonance imaging and computed tomography. Other diagnostic tools may be used in conjunction with these imaging tools as well. These procedures tend to be more invasive, costly, require more time, but can provide more definitive diagnoses of specific neurological disorders. Previous work leading to this point is often done to determine whether a patient has any neurological disorder. Some examples of more invasive procedures include angiography for neurovascular disease, biopsy especially for cancer risk and genetic testing, and

cerebrospinal fluid analysis. These are often all done in a hospital and tend to be associated with patient discomfort as well especially for cerebrospinal fluid analysis [19].

For particular neuro-skeletal-muscular disorders, more specific tests may be used. One example is electroencephalography (EEG) that can diagnose many neurological diseases including seizure disorders, brain damage from head injuries, tumors, and degenerative disorders. This test requires electrodes to be attached to the patient's scalp which conduct a low electrical current to monitor brain activity during different events such as change in ambient lighting, eye movement, changes in breathing patterns. This test can range from an hour in duration to over three hours especially when required for sleep analysis. This test requires the patient to reduce caffeine intake and the cessation of pharmaceuticals that can affect the nervous system. There is also a variation where electrodes are implanted surgically into the skull. For the peripheral nervous system, there is an analogous test called electromyography (EMG) which is used on peripheral nerve roots as well as the brain to measure the correlation between brain and muscle activity under specific events. In particular, EMG is used for nerve and muscle dysfunction as well as spinal cord disease diagnosis. This testing is generally uncomfortable for most patients who undergo it. [34] EMG is also commonly done with a nerve conduction velocity test as well which has many drug interactions and requires the patients' cessation of a broad range of pharmaceuticals [19].

Overall, this traditional diagnostic process narrows down the diagnostic probabilities and allows for accurate diagnosis. However, the neurological disorder-specific diagnostic tests require many hurdles to rule out non-neurological disorders as well such as via a physical exam and neurological exam. Then, the more neurological disorder-specific diagnostic tests also present issues for patients specifically special patient populations like geriatric (O'Brien and

pediatric patients. These first-line diagnostic tools are also expensive, require special machinery and setting, require trained personnel for the machinery operation and result interpretation, time-intensive, and are often not 'first-line' for neurological disorders.

NEUROLOGICAL DISORDERS PATIENT POPULATION

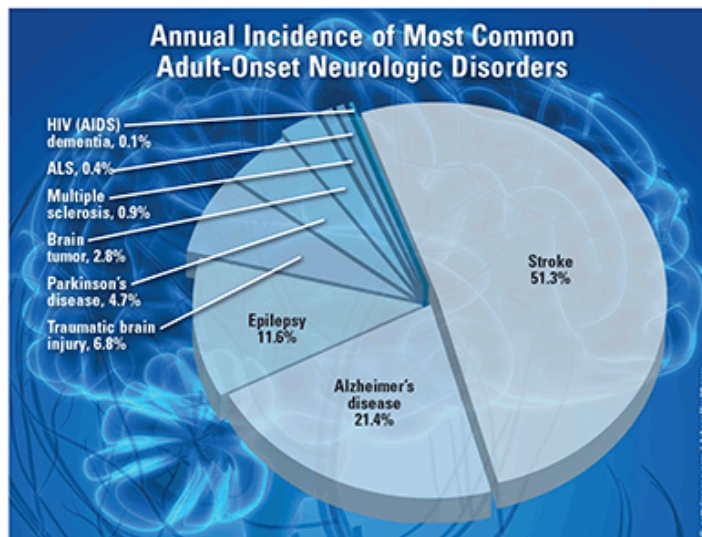


Figure 1 US-based population breakdown of adult-onset neurological disorders [3]

There are many considerations to evaluate when analyzing the population with neurological disorders. The prevalence of neurological disorders is difficult to obtain especially on a global scale. Many of the analyses to obtain an accurate count are completed as case studies. For example, there is a count of the number of neurological disorders in rural parts of Kashmir, a state in India, but it is hard to find an accurate count for the entire state [25]. Finding an accurate count for the country is close to impossible. There is also a case study approach for more specific disease states. For instance, the incidence and prevalence of neurological disorders has been analyzed in conjunction with HIV since the global introduction of highly active antiretroviral therapy [14]. Often these counts are also dated. The most recent World Health Organization report on neurological disorders was published in 2006 while other major publications are from 2000 or earlier [1, 14, 25]. However, it is estimated that 20-30% of the global population is susceptible to neurological disorders [1].

In the United States, there is more data available about the prevalence, but the numbers vary greatly. According to a report published in US Pharmacist, “twenty million Americans experience some form of neuropathy, and 16% of US households contain an individual with a brain impairment. [3]” Another review claimed that “nearly 100 million Americans were afflicted by at least one of the >1000 neurological diseases. [9]” The annual incidence distribution of adult-onset neurological disorders amongst different disease states in Americans is shown in figure one.

These neurological disorders are commonly associated with chronic pain, sleep/wakefulness problems, substance abuse disorders, and cardiac comorbidities. For patients with neurological disorders, there are a number of key demographics that require special attention. They include the geriatric population, mobility challenged patients, athletes

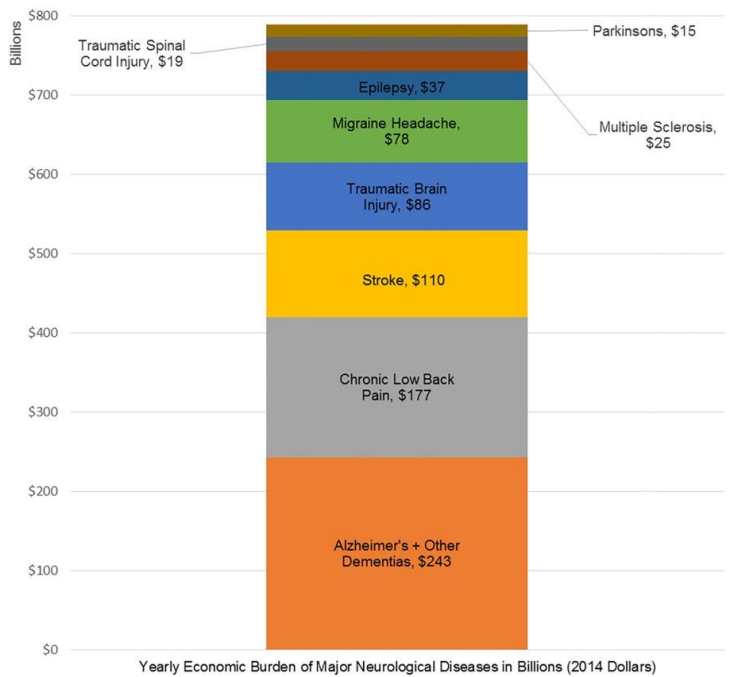


Figure 2 Economic loss due to selected neurological disorders in the United States [9]

particularly pediatric patients, and geographically as well as socioeconomically challenged patients.

The geriatric population is particularly susceptible to neurological disorders. The prevalence of neurological disease in the elderly exceeds the geriatric prevalence of cardiovascular disease and the geriatric prevalence of cancer. Over 35% of Americans over 85 have moderate to severe memory impairment. [3] Additionally, in a review of case studies, elderly patients showed increased prevalence of movement disorders in comparison to the normal population of adults with adult-onset neurological disorders [17, 28], making many mobility challenged patients also intersecting with the geriatric population. These gait disorders tend to lead to more drastic reductions in quality of life and increased mortality along with greater associated health costs [28].

Concussions make up around 9% of high school athletic injuries and around 6% of collegiate athletic injuries “with an incidence of 0.23 per 1000 and 0.43 per 1000 athlete exposures, respectively. [27]” Some sports have a higher risk for concussion than others such as women’s soccer, men’s ice hockey, and football. It appears as though younger athletes are more susceptible to sustaining a concussion. Youth athletes who sustain a concussion recently also show significant differences in general cognitive measure in comparison to youth athletes who did not sustain a concussion recently. It also appears that youth athletes who sustain two or more concussions will have the similar cognitive deficits as a youth athlete who recently had a concussion [18]. This finding shows the significant need to prevent youth concussions and the need for rapid diagnosis of concussions to catalyze immediate neurological attention for sports injuries. One of the major problems in this field is that there is no current way to grade the severity of a concussion on the field. Some factors have been used as historical markers but not

with uniform regulation. These include loss of consciousness, but this does not indicate neither the severity of the concussion nor the length of recovery [27]. There is a significant need for a quantifiable procedure that can determine whether athletic play should continue or if cessation of activity and medical attention is required. These sports injuries may occur in combination with other injuries which require the diagnosis procedure to require as minimal anatomical access as possible as well.

When discussing the global prevalence and incidence of neurological disorders, the literature has primarily been based upon case studies and with varying numbers. This may be due to regional and socioeconomic differences. Additionally, there may not be enough economic support for this research [1, 9]. Within the United States, neurological disease prevalence is correlated to certain socioeconomic sectors. Historically disadvantaged ethnic minorities, women, and patients with lower educational achievement are more at risk for dementia disorders including Alzheimer's disease. These dementia diseases are also positively correlated with increasing age in the geriatric population. Historically disadvantaged ethnic minorities and patients with lower educational achievement are also at an increased risk for stroke. There is also overall significant economic loss particularly in lost productivity which can exacerbate socioeconomic strain [9]. Economic losses may also be reflected in indirect costs, healthcare costs, and other systemic costs. The financial burden is illustrated in figure two. There is also a lack of neurological health care professionals. In the United States, further education to obtain neurological certification can often take six years to complete in a rigorous program. In developing countries, there may not be enough resources and teachers which may lead to slightly faster output of neurological health care professionals but a less comprehensive education [1]. There is also significant social stigma around many neurological disorders such as epilepsy

which can lead to decreased social understanding as well as lower treatment rates [1]. Social competency is an important factor in approaching neurological disorders as well as finding a neutral diagnostic procedure.

In the next section, the identified issues with current diagnostic procedures are approached through the use of an easily accessible central nervous system structure: the visual system.

EYES AS THE WINDOW TO THE NERVOUS SYSTEM

Analyzing eye movements can be insightful for the assessment of neurological functioning. Eye movements have been used as diagnostic tools for over 60 years for many kinds of disorders such as muscular dystrophy, psychotic thought disorders, and autism [12]. The molecular mechanisms of eye movements and their outputting movements can be used to indicate genetic disorders using overlapping molecular derivatives [12].

Class of Eye Movement	Main Function
Vestibular	Holds images of the visual world steady on the retina during brief head rotations or translations (linear movements)
Visual Fixation	Holds the image of a stationary object on the fovea by minimizing ocular drifts
Optokinetic	Holds images of the visual world steady on the retina during sustained head rotation or translations
Smooth Pursuit	Holds the image of a small moving target on the fovea; or holds the image of a small target on the retina that is close to the head, during linear motion (translation); with optokinetic responses, aids gaze stabilization during sustained head rotation
Nystagmus quick phases	Reset the eyes during prolonged rotation and direct gaze toward the oncoming visual scene
Saccades	Bring images of objects of interest onto the fovea
Vergence	Moves the eyes in opposite directions so that images of a single object are placed or held simultaneously on the fovea of each eye

Figure 3 “Functional Classes of Human Eye Movements [12]”, note saccades in particular

There are some key advantages to using eye movements in particular. The eye movements mechanics are restricted to globe rotation while translational movement is negligible. Focusing on rotational movement only simplifies analysis and improves precision. These simplified mechanics also arise from fairly linear and simple connections between motoneuron activity and eye rotation. Also, different kinds of eye movements, shown and described in figure three, can indicate different kinds of attributes about the status of the patient [12].

Eye movements are also physiologically readily accessible by health care practitioners and possible diagnostic procedures and devices. This allows for minimally invasive approaches. This also minimizes problems with other disorders and related comorbidities. Traditional imaging procedures' issues can be reduced as well. For instance, patients with claustrophobia, movement disorders, radiation risk, and/or biological implants such as pacemakers may not be able to undergo traditional imaging procedures especially for first-line diagnostics. Using eye movement also may not requires as much specialized training to access because there is no physiological manipulation required such as for traditional imaging procedures or other diagnostic procedures such as biopsies. Eye movement analysis may also overcome the other issues introduced with current neurological diagnostic procedures discussed earlier.

VISUAL NEEDS AND CLASSIFICATION OF EYE MOVEMENTS

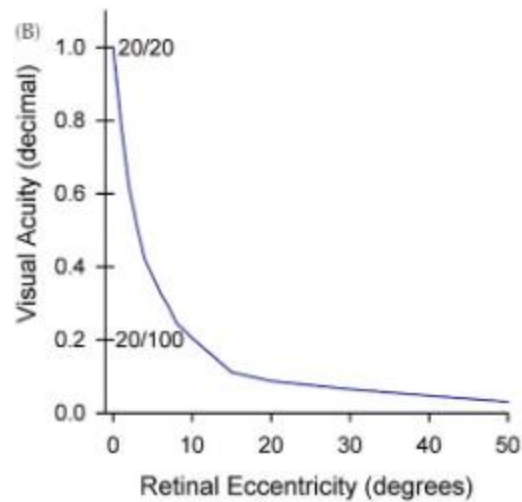


Figure 4 The relationship between the "eccentric displacement of an image from the central fovea [12]" and visual acuity

The overall image must be stable and projected centrally on to the retina, preferably on the macula which has the greatest photoreceptor density. Even two degrees from the center of the macula, the fovea, results in a decline in visual acuity by fifty percent as shown in figure four. The image also cannot move too much or too little. If the images move too little, they become "artificially stabilized on the retina [12]" in which the visual system becomes less responsive to the visual stimuli and vision fades due to adaptation. If the image moves too much, the spatial frequency plays a role in the amount of movement that can be processed by the retina. Higher spatial frequency for example includes images with increased sharp edges. But overall image

motion should be below 5 degrees per second for a stable image stimulus [12]. Otherwise, this results in blurred vision.

Vision can be stabilized in two reflexes which are together known as the “gaze-stabilizing reflexes [12]”. The first way is based upon head acceleration sensing by mechanoreceptors in the “vestibulo-ocular reflexes. [12]” The second mechanism is based on “visually mediated reflexes [12]” in which the brain determines the image speed based on the retinal drift of the image. There are also gaze-shifting eye movements which are particularly important when needing to shift visual attention to an object on the periphery rapidly. The shift also must orient the center of the retina to the most ideal location to view the stimulus optimally [12].

Based on this, eye movements can also be classified into two types where one class deals with keeping a stable image on the retina with steady gaze which can shift steadily to follow the object of interest and a second class deals with the relatively rapid shift of vision towards a new visual stimulus. This can be reflected in the types of eye movements listed in figure three [12]. There may be combinational use especially when approaching the three-dimensional space, but these two classes tend to operate more independently when the visual stimulus is two-dimensional.

The particular eye movement of interest for this model is the saccade and it should be noted that it falls into the second class where the ocular system rapidly “brings images of objects of interest onto the fovea. [12]”

OCULAR MOTILITY MECHANICS

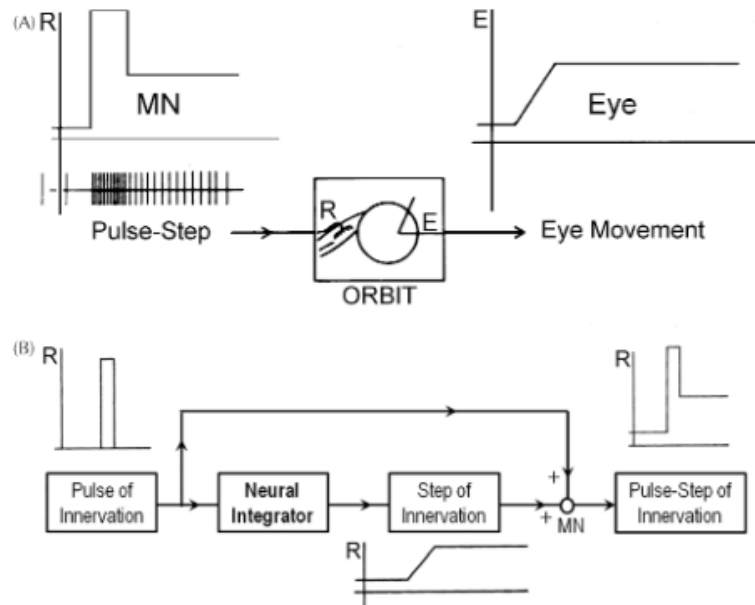


Figure 5 Burst neural activity leads to activated motor neurons which results in eye movement. The type of eye movement modelled here is saccades [12].

The mechanics of orbital movement are based on overcoming viscous drag forces using strong contractions of extraocular muscles. Rapid movements like for a saccade requires an exponentially rapid phasic increase of ocular motor nuclei neural activity which is called the “pulse of innervation [12]”. The eye must be stabilized in that position using elastic restoring forces which restabilize the eye into its optimal, central position. To hold more eccentric positions, more pulses of innervation are required. The integration of these increased pulses leads to an elevated level of overall neural activity. This can be modelled as a “pulse-step of innervation [12].” This allows the eye to rapidly rotate to a new position and hold its orientation in this eccentric position [8, 12].

This can be applied to the rapid movement of saccades. This model is shown in figure five. In part A, the exponential burst of action potentials is shown on the left in the ocular motor neuron (MN) and, on the right, it is shown to result in a saccade. In part B, it shows how the neural integration of an innervation pulse and the pulls itself results in the pulse-step of innervation which is shown in part A to result in the trigger of ocular movement which is represented as angular displacement of E. Here R represents discharge rate of the neuron. [12] Overall this diagram shows the relationship between neural activity and ocular motility.

The frequency of pulse dictates the velocity of the eye rotation. The pulse-step is required to prevent the eye from returning to the central position of the eye and to hold the eccentric position. Therefore, the pulses and the steps must be coordinated for ocular movement. Pulse-step mismatch is a common indicator for pathologies of the eye and the nervous system. Pulse-step mismatch can lead to many presentations such as excessively slow rotation towards the target or drifting past the target. This simplified mechanic model is accurate for two-dimensional visual stimuli. For three-dimensional eye rotations, rotational order can play a more important role [12].

SACCADES AS A DIAGNOSTIC TOOL

Saccades are eye movements where the eye rapidly rotates or ‘jerks’ towards a new object typically on the periphery providing a quick and accurate survey of the external visual environment [8, 12]. Saccades are generally considered to be one of the most well-researched and characterized classes of eye movements and has been extensively mapped out and correlated with different neurological pathologies [8, 12]. The smooth pursuit class of eye movements is not as well characterized for neurological dysfunction whereas distinct deviations from healthy

saccade profiles can shed insight on the diagnostic likelihood of different neurological dysfunctions. Saccades also uniquely show the reflexive arcs of the ocular system.

It should be noted that there is typically about a 100ms to 200ms delay from the original stimulus to the actual saccade enactment which have a duration of 30 to 100ms [8, 12]. This delay is visible in figure five. This is to account for neural processing prior to the saccade. This neural processing and its effects on this delay and actual saccade enactment is used for neurological dysfunction characterization. The ocular muscles are among the fastest in the human body which allows for fast data acquirement. Aside from the characterized neurological dysfunctions and visual disabilities, saccades tend to be normal, rapid, and accurate for most normal patients [12]. Therefore, saccadic eye movement may be a novel neurological disorder diagnostic tool.

INTRODUCTION TO THE SACCADIC SYSTEM

During a saccade, the visual system is closed to other stimuli and the rotation must be completed before another can be initiated. The visual information during the rotation process is not registered and only the final target visual scene is received by the retina. The retina and the motor neurons must act in synchrony. By reducing visual load, the saccadic error in healthy patients is reduced "...to zero [8]". The movement is primarily calculated by the brain via the brainstem, the cerebrum, the mesencephalon, and the cerebellum [8] rather than other eye movement mechanisms which are dependent on the oncoming visual scene to determine eye movement.

SACCADE CHARACTERIZATION CONVENTIONS

Current research focuses on certain target markers to analyze saccades.

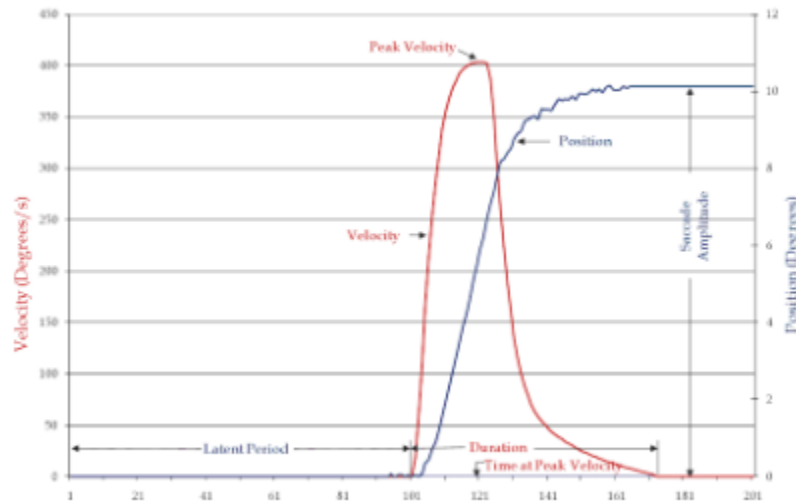


Figure 6 Standard graphical method for plotting saccade data illustrated using an example ten-degree saccade [8]

The first is the latency of a saccade. The latency is considered to be the time required for the central nervous system to determine if a saccade should occur and if yes, the central nervous system must calculate the amount of rotation required and then the corresponding neural activity sequence for pulses and pulse-steps [8]. This occurs from the moment the target is introduced to the visual field to the start of the saccadic movement. The latency can range greatly while other saccadic parameters vary very little from standard ranges. For example, medium amplitude saccades of about five to ten degrees can result in a latency of around 200ms usually. However, latency “can be as low as 100ms or as high as 350ms [33].” This experimental distribution of saccade latency in relation to angular displacement or saccade magnitude is shown in figure ten. Saccade latency distribution is of great research interest currently. Significant deviations may show more unique profiles indicating specific higher-level brain processing statuses, even higher

than the superior colliculus and brainstem. This would allow for even more fine-tuned correlations between saccadic movement and neurological status. However, this point is controversial. Others assert that there is no relationship between latency and saccade amplitude and that it is “unimportant” and should be considered as an implicit factor in saccadic analysis [8]. Further research is required for definitive discussion of latency and its role in saccadic analysis.

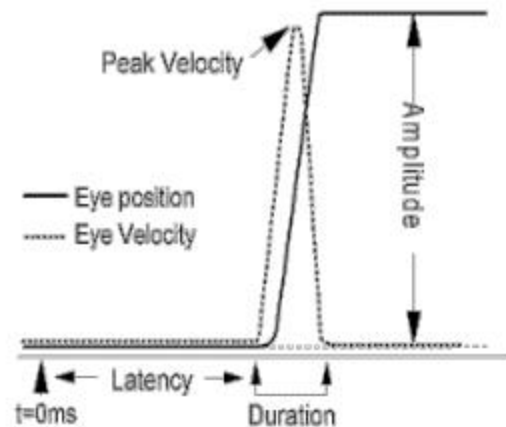


Figure 7 General saccadic parameters of interest shown on a saccade plot [33]

The second key data required for saccade analysis is peak velocity of the rotation. Higher peak velocities tend to be associated with shorter saccade durations and lower peak velocities tend to be associated with longer saccade durations [8]. Trajectories may vary depending on environmental and internal conditions even in reaction to the same visual stimulus [8]. Often this can be calculated as the gradient of the displacement of eye rotation over the time of a saccade event. The peak velocity reached is found at the maximum point of the saccadic velocity curve spike which is usually around half of the way through the saccadic event [33]. Some neurological dysfunctions may result in the reduction of peak velocity and these events are referred to as slowed saccades [33].

Saccades may be analyzed through plotting target data against saccade magnitude. Saccade magnitude is typically the angular displacement of the rotation which may be given either in degrees or in arc minutes [33]. Some data that is plotted against saccade magnitude is peak velocity, saccade duration, and saccade latent period [8]. A standard saccade plot is shown in figure six. A generalized version of this plot is shown in figure seven. It shows the peak velocity curve over time as well as the angular displacement over the duration of the saccade. Angular displacement can be minimally less than a degree such as in microsaccades to 45 degrees towards either the nasal or temporal directions. Angular displacement may also be referred to as amplitude along with overall saccade amplitude as shown in figure seven [33].

Angular displacement may sometimes be used to calculate a 'gain' for the function which is the ratio of the actual experimental saccade magnitude divided by the theoretical desired saccade magnitude. This shows the saccadic accuracy. For example, if the gain of the function was less than one, then the movement was too small which is referred to as hypometric which indicates that there is an overall neurological dysfunction in which neurological computed muscle movements are short of the desired target. If the gain was over one, then the movement

$$v_{\max} = \alpha \left(1 - e^{-\frac{x}{\beta}} \right)$$

Figure 8 Equation relating peak velocity to saccade magnitude for magnitudes greater than fifteen degrees yielding a non-linear relationship [8]

was too large for the stimulus which is referred to as hypermetric which indicates that cognitive calculations of muscle movements are too large for the desired target. These two states of neurological computational pathology can be indicative of a number of disease states from congenital to lesion or drug-induced origins. Saccade dysmetria refers to when saccadic movements are inaccurately too large or small in magnitude [33].

As mentioned previously, peak velocity typically occurs around the halfway timepoint of the rotation when the saccade magnitude is less than fifteen degrees and then tends towards a constant for larger saccade magnitudes [8]. This relationship has been fitted to an exponential function for the non-linear region. This equation is visible in figure eight where maximum velocity is shown to equal a constant multiplied by one minus the natural base to the power of the negative of the saccade size divided by another constant. α represents the steady-state portion and β represents a time constant [8]. These constants are determined to minimize the error of the function and vary from saccade to saccade. A step function visual input can help to determine

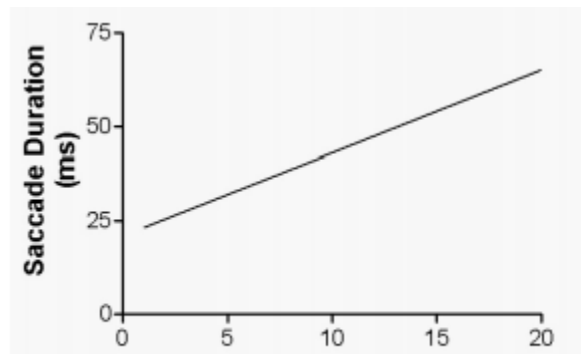


Figure 9 Saccade amplitude and saccade duration show a linear relationship (here it is it to 2.2 (saccade amplitude) plus twenty-one is equal to the saccade duration in milliseconds [33]

whether this relationship between peak velocity and saccade magnitude falls in the linear or non-linear regions. Therefore, visual stimuli are experimentally modelled to provide this step input [8]. Recall that the actual neurological driver of the saccade is a pulse-step and not just a step function.

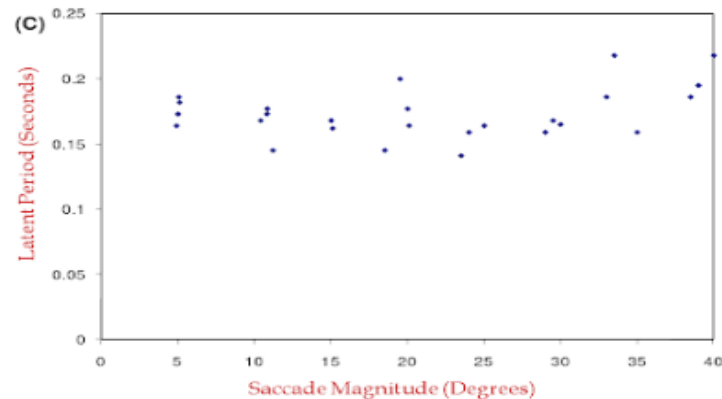


Figure 10 The current understandings of the relationship between experimental latency and saccade magnitude [8]

Another important endpoint is the time it takes to complete the saccade event which is referred to as the duration [33]. Usually this is obtained via the velocity curve rather than the displacement curve. Due to the high velocities and computation times for saccades, the durations of saccades are typically very short and usually measured in tens of milliseconds [33]. The duration of the saccade can vary based on the degree of rotation where saccades less than five degrees lasting ~30ms and saccades with larger degrees of rotation lasting up to 100ms [8]. Saccades with magnitudes greater than seven degrees also show “a linear relationship between amplitude and duration [8].” Some sources assert that this linear relationship can be shown in saccade magnitudes as small as 1 degree. This assertion of linearity starting at one degree is

graphically shown in figure nine. This should also be kept in the context of the linear to exponential peak velocity relationship with saccade magnitude for saccades less than and greater than fifteen degrees respectively. The exponential relationship considerations, shown in figure 8, are often avoided in saccadic profile analysis by designing visual stimuli that have saccade amplitudes with a gain of 1 below fifteen degrees [33].

The duration also has a neurological role. It takes around 80 milliseconds for the visual cortex to receive any visual information [33]. This is another strong support for the important neurological basis of saccades. They cannot be changed in the middle of the event and must complete the calculated trajectory. If new visual information is received, such as a change in the position of the stimulus, an entirely new saccade must be calculated and completed. These saccades immediately following the original saccade may be referred to as “corrective saccade[s] [33].” If the duration of the saccade is too long or short, this is often reflected in the velocity curve shown on the saccade plot.

SELECTED SACCADE AND NEUROLOGICAL DYSFUNCTION CORRELATIONS

There is a neurological-basis for saccades. Based on the key saccadic parameters discussed, diagnostic profiles can be used to compare eye movement to neurological dysfunction. Some selected movement-based neurological pathologies are presented in figure eleven along with each key saccadic parameter. A diagnostic decision chart is also shown for selected pathologies in figure twelve. In figure eleven, the terms hypermetric and hypometric refer to the saccadic magnitude gain being above one or below one respectively. The hypokinetic and hyperkinetic refer to types of movement disorders. Delayed saccade initiation can be measured from latency. Saccadic velocity is obtained from the velocity curve. Square wave jerks can be

seen in the slope of the saccade plot's displacement curve. Saccadic intrusions also refer to movement deviations during the steepest part of the saccade plot's displacement curve. The covered pathologies are Parkinson's disease (PD), multiple system atrophy (MSA), progressive supranuclear palsy (PSP), corticobasal degeneration (CBD), opsoclonus-myoclonus ataxia syndrome (OMAS), Huntington's disease (HD), neuroacanthocytosis, spinocerebellar ataxia (SCA types 2,3,6, and 8), ataxia-telangiectasia (AT), and ataxia with oculomotor apraxia (AOA types 1 and 2). The plus indicates the presence of the saccadic abnormality [29]. In the decision chart in figure twelve, there are a few more pathologies: corticobasal syndrome (CBS), Friedreich's ataxia (FA), gaze-evoked nystagmus (GEN), Niemann-Pick type C (NPC), and vertical supranuclear gaze palsy (VSGP).

Movement disorders	Delayed saccade initiation	Slow saccadic velocity	Hypermetric saccades	Hypometric saccades	Square wave jerks	Saccadic intrusions during pursuit
Hypokinetic						
PD ¹				+ ²		
MSA			+	+	+ ²	+
PSP ²		+ ³		+ ³	+ ⁴	
CBD	+	+ ⁷				
Hyperkinetic						
Myoclonus						
OMAS						+ ⁸
Chorea						
HD ⁹	+	+				
Neuroacanthocytosis ¹⁰	+	+				
Ataxia						
<i>Dominant form</i>						
SCA2		+				
SCA3 ¹¹						
SCA6 ¹²						
SCA8			+			
<i>Recessive form</i>						
AT ¹³	+ ¹⁴			+		
AOA1	+ ¹⁴					
AOA2 ¹⁵	+ ¹⁴					

Figure 11 Summary of saccadic profile characteristics of several neurological disorders [29]

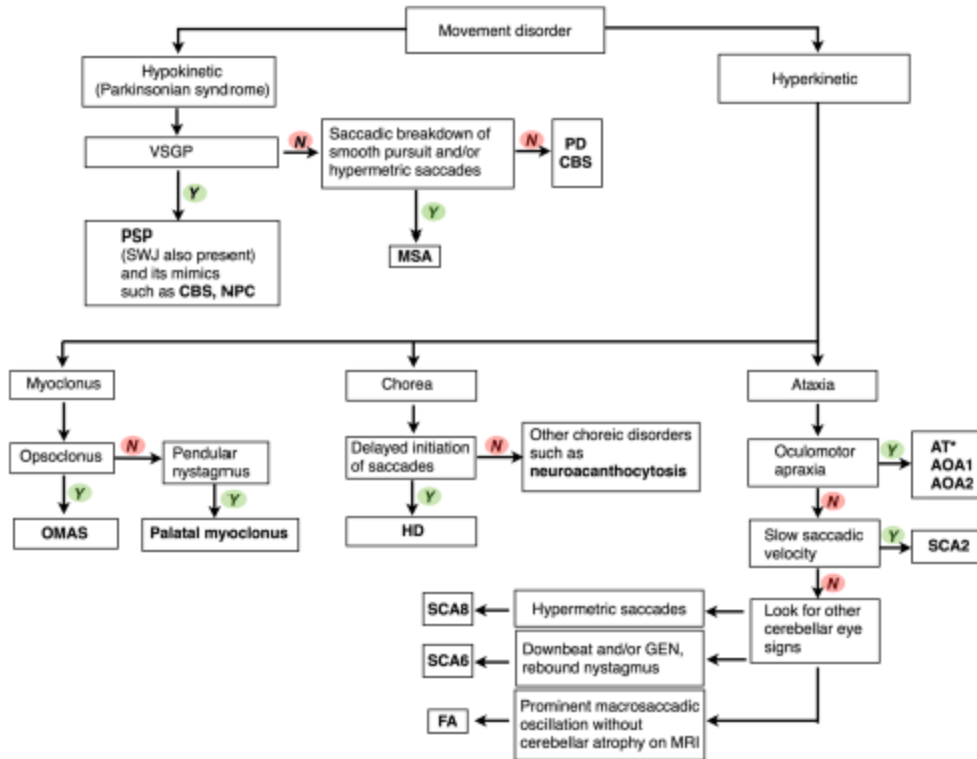


Figure 12 Decision chart for saccade-based neurological analysis [29]

CURRENT EYE MOVEMENT RECORDING METHODS

Ocular motility can be recorded by various procedures. Some include “electrooculography, video oculography, scleral search coil and infrared oculography [8].”

Typically, the visual stimuli used to trigger the saccade tends to have high contrast objects and backgrounds. One example experimental visual stimulus is using a horizontal array of LEDs where only one LED is active at a time. The active LED switches off and another LED simultaneously turns on which triggers a saccade of a predetermined magnitude [8]. The background is typically high contrast with the saccade-triggering objects. Continuing the LED example, the background is dark to contrast with the lit LEDs.

An important feature of experimental setups is that saccades tend to be restricted to a particular axis in order to reduce confounding effects of testing both horizontal and vertical visual attention simultaneously as well as having to consider mechanical torsional factors. Conventionally, saccade visual stimuli tend to present as horizontal triggers as horizontally stimulated saccades are best profiled of the three possible directional movement triggers, i.e. horizontal only, vertical only, and diagonal (horizontal and vertical components) [8].

One current method of measuring eye movement is to use electrooculography in which the permanent potential different between the fundus and cornea of around one millivolt is measured. Small voltage shifts can be ascertained by using carefully placed electrodes. However, this signal is not isolated for just optical movement. It can change as the eye adapts to dark settings which can show more information about retinal health but not as much about neurological status. It is also overall affected by metabolic changes in the eye, can migrate within the experiment, and may show spurious signals. This procedure is cheap and generally non-invasive but is not reliable. This is frequently used by clinicians and would not be useful for the general public [32].

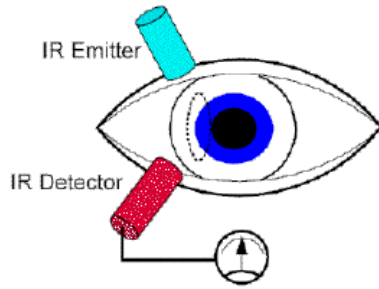


**Figure 13 Schematic
diagram of experimental
infrared oculography set-up
[32]**

Another method is infra-red oculography, shown in figure thirteen. This measures the amount of infrared light reflected back by the eye. This can vary based on ocular position. This is used in many commercially available eye trackers. The infrared light is not visible to the user, so it does not provide discomfort or distract the patient. The spatial resolution is generally very good and can be accurate up to even an order of a tenth of a degree. The infrared system also has a very good temporal resolution of around 1 millisecond. This is better for horizontal saccadic movement than vertical movement however. Blinking can also result in inaccurate results as the eye retracts slightly after blinking which can change the light reflected for a short time after. [32]

An additional method of eye movement detection is to use scleral search coils. The coils movement in a magnetic field creates a voltage. In this method, the scleral coils are attached to the eye and voltage changes are recorded as the eye moves. The small coils can be inserted into the eye via a contact lens or annulus and exits the eye at the temporal canthus. This is inserted into the eye after administering local anesthesia. Then the field is generated by placing two field coils on either side of the head. This allows for both horizontal and vertical saccade detection at

once if two sets of field coils are used. Scleral search coils can also be used to detect microsaccades and provides the best resolution of current eye movement recording methods. However, this method is extremely invasive and uncomfortable to the patient. It is rarely used in clinical settings and is almost exclusively used for research purposes in animal-models. [32]

There are also some image-based methods. These typically involve Purkinje images which are images of the eye which show a given object reflected in the image. For example, glint from an artificial light source may be used to determine positional values. The reflection of light at various points in the eye around the lens and cornea result in these glints. This method is explored in this project in the alternative design section. Another method used in videos and other software techniques is to use the position of the pupil based on the exact center of the image. The issue is that pupil detection may be difficult depending on the patient as well as experimental conditions. The center of the image may also vary from frame to frame if the experimental conditions are not stable. Pupil detection is also often found via image filtering which is also discussed in the alternate design section. Another issue is that, in some cases, this pupil detection is not automated and requires the manual selection of the pupil in a given image or video frame. There may be combined filtering and pupil surveying of the image which reduces the number of pupil candidates for the experimenter. However, the final pupil choice must be specified by the user manually [37]. This is computationally and temporally too expensive. Eye positional analysis must be as automated and easy to use as possible. This approach to this positional marker may not be the best for current needs.

Therefore, there is a need for an eye detection technique that is low-cost, mobile, reliable, accurate, and does not require extensive training or a health care practitioner to administer. There

also is a need for a system that can also accurately translate this to saccade plots in order to have accurate neurological diagnostic value.

CURRENT PITFALLS OF OCULAR DETECTION AND MOTILITY ANALYSIS

Some problems with current ocular motility analysis methods are issues with identifying certain eye structures, economic cost, issues with identifying certain pigmentation schemes, computational cost, and generally research-restricted administration of ocular motility tests.

First, usual eye detection requires standard settings and well-lit environments. [37] The use of filters requires high contrast lighting. Methods based on image center also require stable centers throughout the eye movement. These cannot dynamically obtain the positional eye values throughout the saccadic movement. Additionally, if the experimental conditions are poor, the eye detection may be for too general a field for accurate saccade detection. For example, current methods may be able to detect eyes from a face but unable to detect finer pupil or iris movement throughout the saccade. This will result in artificially too small displacement values and inaccurately reflect ocular motility.

Patient pigmentation or structural characteristics may also confound results [10]. For example, filtering methods may not be able to detect eyes of some patients of Asian descent [37]. This lack of accurate facial detection in racial minorities has been a key hurdle of facial detection. Prominently, Apple and other technology companies have come under fire for low thresholds in facial detection for non-Caucasian eye structures and other facial characteristics [13]. Darker eye colors and skin tones may also lead to confounding results in even well-known eye detection methods [11]. Pixel detection of eye locational markers is typically tested in Caucasian male populations [11, 13, 37]. In the papers reviewed, these are often given as

secondary limitations of the eye detection method. In a widespread facial detection software comparison, the New York Times found that women were less likely to be accurately detected than men. For Caucasian men, the software was accurate for up to 99 percent of cases. For darker skinned women, the detection error rate was almost 35 percent [13]. There needs to be “algorithmic accountability” as Joy Buolamwini is quoted [13]. In machine learning algorithm-based approaches, the same detection errors are present. There is a clear need for more accurate detection methods to include more pigmentation and structural paradigms of potential patients.

PROPOSED SACCADE DIAGNOSTIC MODEL

The proposed solution is to find a low-economically costly and low computationally-costly solution to analyze saccadic movement from eye images in order to use as a first-line diagnostic tool. This solution will focus on how to obtain key saccadic movement parameters based on a smart phone video recording of eye movement. The key purpose of this exploration is to identify a method to identify ocular topological markers to extract ocular motility information. This solution must also be able to address considerations of generalizability to identified historically underserved or key target populations such as racial minority populations, geriatric populations, pediatric populations, and socioeconomically challenged populations.

Some information about corresponding experimental conditions will be discussed. However, detailed final hardware set-up is discussed elsewhere and may be requested from the author.

METHODS, DESIGN, AND EXPERIMENTAL PROCEDURE

OVERALL EXPERIMENTAL OBJECTIVES

This project aims to create a system to analyze images of eyes captured on a smartphone-device and detect ocular position over the duration of a saccadic event which is stimulated by a visual trigger also displayed on the smartphone-device. The specific hurdle is the detection of eye position obtained from the smartphone front-facing camera. In this section, the experimental set-up will be discussed as well as some alternative designs leading to the final design.

OVERVIEW OF EXPERIMENTAL SETUP FOR SACCADE ANALYSIS

VISUAL STIMULUS

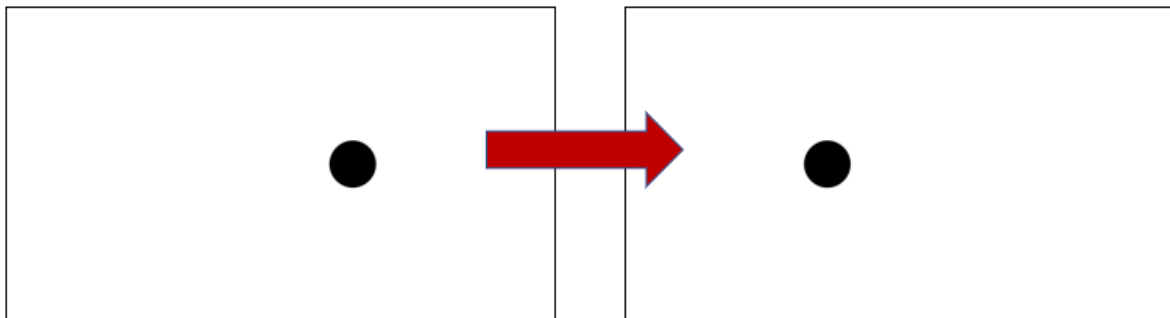


Figure 14 Representation of visual stimulus switching from central position (stage two) to eccentric position (stage three) based on a particular user's smartphone orientation in the final hardware device.

The visual stimulus is based on three visual settings: the first portion is a blank reset screen, the second portion is a centered black dot on a white background to provide a visual prompt to center the eye and projection onto the retina, and the third portion is a black dot with a variable horizontal displacement from the center to prompt a rapid movement of the eye to an eccentric position and projection onto the retina.

USER DATA INTAKE

User data was recorded based on a video recording through the front facing camera of the smartphone device. This recording occurred as the visual stimulus was playing using an auxiliary app called Background Video Recording that allowed the camera to be used while another app was open. This app is available for download on the Google App store and stored one-minute videos of user eye movement for around 30MB. There needs to be a set amount of free storage on the smartphone for this system to function correctly.

USER DATA ANALYSIS

Two codes were created for user data analysis: *eyetest2frames* and *imagesetanalyzer*. Both of the explicit programs are provided in the appendix of this report. *Eyetest2frames* intakes a video of user eye movement and extracts the frames of the video, storing the frames in a folder in a specified directory. This also obtains metadata about the video such as duration and frame rate. *Imagesetanalyzer* detects the iris position in each frame extracted in the file made by *eyetest2frames*. The iris position is converted to angular displacement and then the peak velocity is calculated as the gradient.

This software was packaged to be as modular as possible. *Eyetest2frames* can extract the frames and metadata of any video. *Imagesetanalyzer* is more specific to eye movement videos.

Each allows the user to specify the exact file and directory in order to be as customizable and interchangeable as they can be. This allows researchers to break out video processing and data analysis as they desire.

DATA OUTPUT

The angular displacement and peak velocity data are then plotted in the appropriate conventional units of degrees per millisecond and degrees per second respectively over the duration of the eye movement video in millisecond.

The resulting graph is referred to as a saccade plot. It is the most appropriate based on saccade research conventions for analyzing saccadic profiles for comparison between healthy patients and neurological dysfunctions. This information sets up the system for the best comparison between current saccade experimental set ups and this device as well.

In this project, the focus is on the positional analysis of the eye during saccadic movement. The final design is an iris detection approach in imagesetalyzer which proved to be accurate for saccade analysis and met the objectives.

ALTERNATIVE DESIGNS

The target optical topological markers for this project have transformed throughout experimentation. Initially, artificial glint position and pupil position were considered as a system to determine optical motility where the distance between the pupil and glint would be calculated and obtained over the saccade duration. Then, the lacrimal caruncle was considered as a topological constant to compare pupil position to over glint position due to concerns of glint irregularity throughout experimentation and hardware changes as well as between different eye structures. There was also a concern that artificially inducing a glint with an additional light source may put a strain on the patient's eyes and confound results. Eventually, the iris was identified as a key locational marker for eye movement. This exploration resulted in the final design.

IMAGE BINARIZATION

For alternative design considerations, there were various image processing techniques explored in MATLAB. For the first runs, a stock image of the eye was used for a proof-of-concept. The image was in the truecolor format which can store 24-bit information of RGB values whereas an RGB-specified MATLAB image can only store up to 16-bit information of RGB values. This truecolor format had to be converted to the RGB format in order to be manipulated in many ways using MATLAB's host of image processing functions. The main alternative to the optimal design was to approach the image as a binary intensity image, referred to also as a binarized image in this project. The truecolor image was then converted into grayscale. From there, the image was binarized. Each pixel was given a true or false value leading to the expression as either 0 or 1.

Binarized images provide concrete value maps for an image depending on whether a base level is reached or not. The higher the binarized level, the image becomes closer to black. The lower the binarized level, the image becomes closer to white. This acts as an extreme contrast system. This would allow the program to continue to filter until the desired point (i.e. the pupil) is narrowed down and the center can be determined.

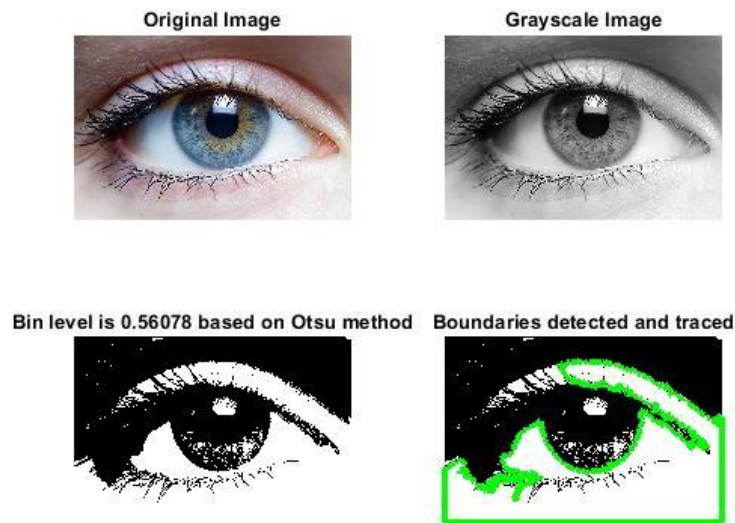


Figure 15 (Clockwise starting at top left) original truecolor stock eye image, grayscale conversion of original truecolor stock image, binary image produced via Otsu’s method of binarization, boundary filter applied using built-in MATLAB functions

All images in figure fifteen except for the original are all binarized versions of the grayscale image. Image three shows an ‘automated’ binarized image. The binary level of the image is determined by the Otsu’s method which allows the image to have an optimal threshold value determined by the overall image composition. Binary images allow MATLAB to detect boundaries. This boundary trace is plotted over the Otsu’s method derived binary image in figure sixteen

Boundary traces with lower binary level 0.4



Binarized with even lower level of 0.15



Figure 16 Binarized images with different minimum levels for value allocation leading to higher contrast images (all figures made in MATLAB by the design team).

In the upper portion of figure sixteen, a binarized image is shown with a level manually set at 0.4 and with a boundary trace plot applied. The pupil is better detected by the trace at this level, but the reflected light is difficult to pick up. In the lower portion of figure sixteen, a binarized image

is shown with an even lower manually set level of 0.15 is displayed. At this level, the pupil contrast is highest, but the built-in MATLAB boundary tracer is unable to detect it.

The main positive aspect of this design is that this method uses many built-in MATLAB functions that can be easily used together. However, there are some issues with this method. Images seven through eight require manual inputs depending on the image which would fail to support the objective of real-time data analysis. This process requires the use of many image conversions and filtering resulting in decreased computational efficiency. The appropriate eye positional markers are also not detected. The ease of conversion between images as well as some automation is something that future designs also hold in common. The goal is to create a universal analyzer that can pick up the ocular positioning markers in a superior manner.

HIGH PASS IMAGE FILTERING AND OTHER FILTERING ALGORITHM IMPLEMENTATION

Another tool that was explored for identification of the pupil, glint, or other motile ocular locational marker was the MATLAB capabilities for using high pass filtering for image manipulation. This filter provides outlines of major boundaries in the image.



Figure 17 Example of a Gaussian high pass filtered image [7]

This requires less computational demand than the binarized image approach. It provides a slightly more straightforward way to isolate boundaries without converting it between many different color values such as a truecolor format to RGB format to grayscale format. This also will be easier to use on many different kinds of input data whereas some previous binarized images required the manual entry of appropriate binary levels for the filtering. The high pass filter development is still ongoing. Further progress will be updated as per the timeline provided below.

Basic experimental smartphone-captured photos were run for various eye filtering methods. Below are the results of filtering on one preliminary experimental set up for obtaining eye images:

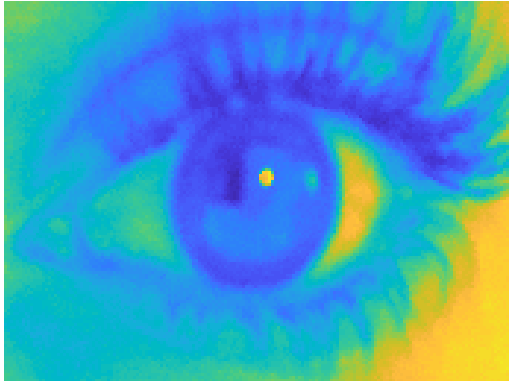


Figure 18 Original eye image

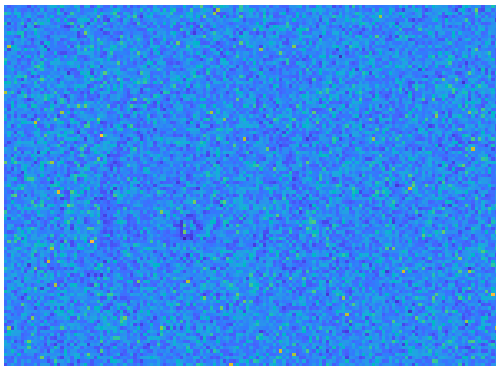


Figure 19 Standard Deviation

Filtering of Entropy Filter

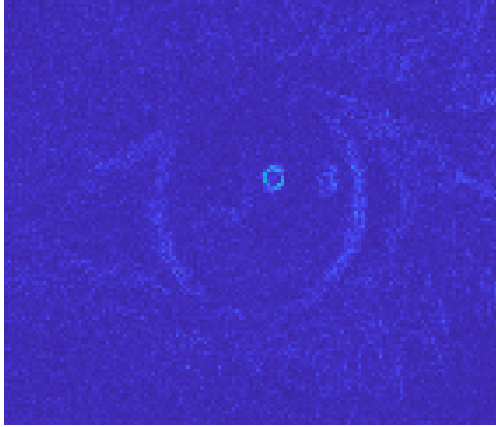


Figure 20 Standard Deviation Filter

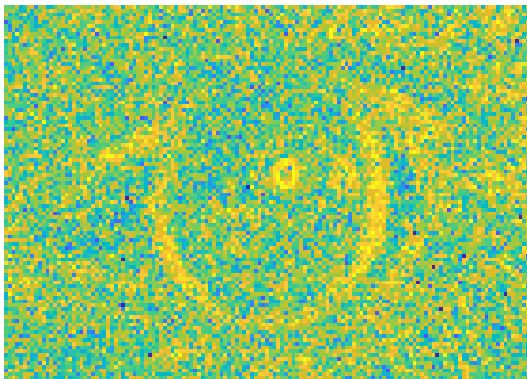


Figure 21 Entropy Filter

The filtering methods were able to detect the glint occasionally as shown in the above set of data. The use of multiple filters also allowed the team to try to analyze what were the best imaging conditions for experimental devices moving forward. However, the glint detection was not consistent and often failed. The glint that was identified also could have an irregular shape depending on the experimental conditions. This was in particular due to the fact that the hardware device had not been created until much later in software development. The glint also did not always

have enough contrast with the rest of the eye. The glint location could not be identified automatically which made the process too labor intensive. The first thought was that this method needed to have increased contrast to work which is shown in the dot matrix supportive alternative design. However, overlaying did not work to obtain the glint. On top of this, again, there was no way to obtain locational metadata about the glint.

The filtering process also did not work on everyone's eye shape. Through this design, more population inclusive methods were sought out. It was clear that there also had to be another ocular positional marker to use. There was some discussion about using the lacrimal caruncle or tear duct through a machine learning process of searching for a particular angle formation. However, this idea was not pursued as it clashed with the goal of searching for more population inclusive methods. The angular measurement of the lacrimal caruncle varies greatly from individual to individual.

AUXILIARY DOT MATRIX OVERLAY

Another alternative design method was to overlay a dot matrix on top of eye images and then use in conjunction with the above filtering methods or binarized image boundary methods. The dot matrix was thought to mask noise in the image and increase contrast to higher contrast regions such as the glint and the pupil which were respectively considered the brightest and the darkest region of the target user eye images from the experimental set-up.

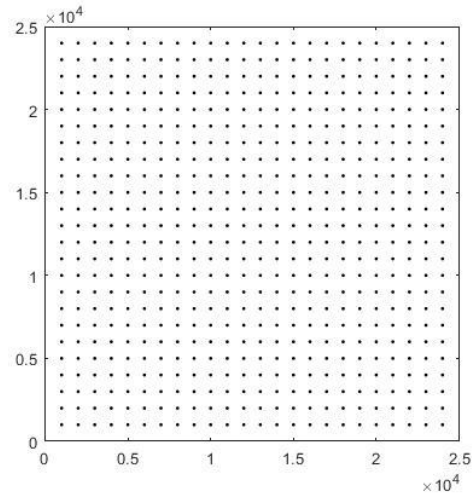


Figure 22 Dot matrix for increasing contrast in image processing

However, the overlay of the dot matrix did not improve glint detection and its overlay could not be automated by the team. The filtering mechanism was not feasible for this project.

INTRODUCTION TO MACHINE LEARNING

Machine learning is an area of research in which computational systems perform tasks without receiving explicit instructions [20]. This may be considered as a subsection of artificial intelligence. This general concept can be applied to many different processes. Some examples of machine learning-based approaches for image processing include facial detection software used in popular social media networks and identification of indexed images on search systems. This approach has many interesting biomedical applications as well. This may be used to automatically detect abnormalities in histological samples, identify unique regions of brain activation given fMRI results, and reconstruct three-dimensional models based on two-dimensional images [20]. The use of a specific image processing tool is used in this project to automate the detection of the iris in order to obtain optical positional values.

CIRCULAR HOUGH TRANSFORM

HOUGH TRANSFORM

The Hough transform is an imaging processing method that attempts to detect geometric features based on pixel value differences in comparison to regional pixel differences. The primary origin of this method was for generally detecting edges. The binary edge detection method shown in the alternative designs is related to this process. The key feature of this process is that it can accurately detect arbitrary features probabilistically given a minimal list of feature parameters. It can be as specific or generally as the situation requires. It can be considered a very generalized form of feature detection and has been used for many different geometric shapes [4].

$$r^2 = (x - a)^2 + (y - b)^2$$

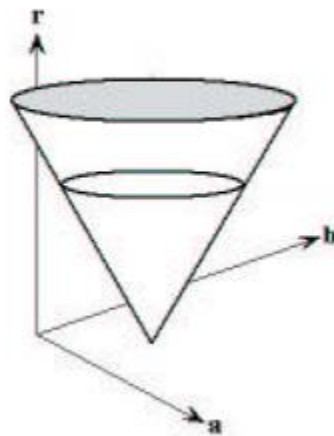


Figure 23 Circular Hough Transform parameter space in relation to the standard geometric equation for a circle (Modified from Pederson, et. al)

APPLICATION TO CIRCLE DETECTION

The Hough transform can be applied to circle detection. This can be done by applying the standard equation for a geometric circle on to an image given a radius. The parameters a and b are positional markers for the x and y directions respectively. Given a desired radius range, the transform can output the positional parameters. The reverse can be done as well although it is less common. The specific mechanism of this Circular Hough Transform is discussed in its presentation by the MATLAB built-in function, `imfindcircles`.

PREVIOUS EYE DETECTION WORK DONE BY HOUGH CIRCULAR TRANSFORM

There has been work done on using Hough circular transform for eye detection [10]. These have primarily been research based and not commercially available for the public. There have been some issues in the implementation on underserved pigmentation and structural patient feature analysis discussed earlier in limitations of current eye analysis. These algorithms are also typically used on still, individual images [10], rather than the desired video analysis. There have also been very few explorations of this form of eye detection for saccadic analysis. Previous work on this intersection of the Hough circular transform and saccadic analysis was also only run on computationally powerful devices as proofs of concept [30]. This project also worked on building Hough Transform tools without using the built-in `imfindcircles` function using Canny edge detection. However, it was unable to detect the iris accurately using experimentally captured images.

MATLAB has a built-in Circular Hough Transform function called `imfindcircles`. The minimized function takes in an image `A` and a specified radius or radius range and outputs the positional values such as the pixel location, radius of the detected circle, and the number of circles in each image. This function works by determining all the edges in an image. Then, using each edge point, circles of the desired radius are sketched between the points. Each pixel is probabilistically ‘voted’ on by whether it falls within a circle or not. The probability is kept track of in an accumulator array [23]. This accumulator array calculation can be configured in two different ways [2, 35, 6] such as two-stage or the default phase-code. This can be specified as a parameter passed to `imfindcircles`. In this project, the default phase-code version is used. Each successful chance of being part of a circle of the desired radius increases the pixel’s value in the accumulator array. Then after this stage is done, the maximum values of the accumulator array are obtained. In this way, the pixel values that are most likely to be in a desired circle are obtained.

For this project, the radius of the iris must be obtained (for example through `imtool`, a measuring tool built-in to MATLAB) and an eye image must be passed to `imfindcircles`. In a standard experimental setup, iris size will not range greatly. However, this tool allows for a range of radius to be measured which increases the generalizability of the program. The image can be either a grayscale image, truecolor image, or binary image. This cuts down on computational time. The radius range can be passed to the function as a two-element vector of a minimum radius value and a maximum radius value. The object polarity can also be indicated. This is to denote whether the expected circle will be dark as in darker than the background or bright as in brighter than the background. In this project, ‘dark’ was denoted. Another factor that can

contribute to specificity is ‘sensitivity’. This is a number that can range between 0 and 1 where increasing the sensitivity factor results in the detection of more circular objects even those that are partially obscured or perhaps weakly circular in character. This is a balance between making the program specific and minimizing false detection. The final input variable that can make `imfindcircles` more specific is ‘Edge Threshold’ which indicates what the threshold for edge pixel gradients should be. This can also range between 0 and 1. Higher edge thresholds indicate higher gradient thresholds for pixel edge designation which may result in fewer circles being detected. Edge threshold values and sensitivity factors varied in this project depending on experimental configurations.

The x-axis positional values from the centers output of `imfindcircles` was used to convert the pixel values to angular displacement using the fixed distance the user was from the visual stimulus screen as well as saccade velocity.

EXPERIMENTAL IMPLEMENTATION

In the experimental implementation, there were some points of consideration.

The first was the decision to determine which topological marker to use for positional analysis. The pupil had been presented as a conventional marker for saccadic analysis. However, the use of novel, computationally inexpensive methods showed that the Hough Transform best functioned when obtaining the largest predicted circle given in an image of the eye. Therefore, the iris was easier and more accurately detected than the pupil. It also does not change in radius given light exposure whereas a pupil may dilate or contract depending on environmental factors. The iris detection also minimized previous work’s issues with iris pigmentation confounding pupil detection. There may be slight benefits from detecting the pupil rather than the iris for

greater accuracy for microsaccades. However, the trade-off between overall accuracy and generalizability makes the iris a more ideal candidate for positional analysis.

As the iris moved towards the corner of the eye, it forms a more elliptical shape than circular. This may result in the overlap of two detected circles instead of the desired one. However, this can be corrected by averaging the centers of both of the obtained circles for accurate locational detection.

Initial concerns about experimental setup focused primarily on the presence of a light source during testing. In previous alternate designs, such as filtering, there needed to be enough contrast between the optical topological markers for analysis. This detection method functioned appropriately in lower lighting conditions which reduced the strain on the user's eye. Further finalization of a stable hardware encasement may reduce noise in positional analysis. However, based on the initial explorations of the system, the saccade signal noise is currently minimal enough to accurately reflect accepted healthy saccadic parameters for healthy patients.

RESULTS

FINAL IMAGESETANALYZER PROGRAM

%%%

%%%

%%%

%%%

%Senior Design Team 8

%Written by Maigh Attre and Alexandra Liberti

%%%

%%%

%

%This code takes a file with images labelled with file name suffix of

%'Frame-'

%

%Each image is passed through a Hough transform-based algorithm,

%imfindcircles, and determines the location of each circle in the image.

%

%This should detect major eye locations throughout the set of images and

%store these positions.

%

%These pixel values are converted to centimeter values. The screen distance

%and the eye locational markers are used to determine the angle of saccade

%throughout the image set.

%

%This angle is then plotted against the duration of the original video

%

%For correct functioning, please run eyetest2frames prior to this with the

%appropriate video and use its output to analyze. There are some global

%variables used from eyetest2frames. If you do not want to use

%eyetest2frames first, modify the final plotting line and input the video

%duration manually for the variable v.duration.

%

%%%

%%%

```
%%%%%%%%%%%%%%%%%%%%%%%%%%%%%%%%%%%%%%%%%%%%%%%%%%%%%%%%%%%%%%%%%%%%%%%%
%%%%%%%%%%%%%%%%%%%%%%%%%%%%%%%%%%%%%%%%%%%%%%%%%%%%%%%%%%%%%%%%%%%%%%%%
```

```
image_dir=uigetdir([]);
```

```
%choose a folder of images with the appropriate naming syntax
```

```
frame=dir(fullfile(image_dir, 'Frame*.jpg'));
```

```
%REMEMBER TO PUT IN USER DISTANCE TO INTERFACE SCREEN AS THE GLOBAL
```

```
%VARIABLE SCREEN DISTANCE
```

```
%also remember to put in stimulus distance based on your screen as well
```

```
global screendistance stimdistance
```

```
screendistance= 10; %cm
```

```
stimdistance = 5.4; %5.4 on my Samsung S8 in cm%11.43 on Alex's laptop %cm
```

```
%holds all locational values obtained from analysis
```

```
eyepositionarray=[];
```

```
for k= 1:numel(frame)
```

```
    %opens up each frame captured
```

```
    filename=fullfile(image_dir, frame(k).name);
```

```
    %reads each image
```

```

rgb = imread(filename);

%converts to greyscale

gray_image = rgb2gray(rgb);

%runs Hough circle transform to detect eye location throughout the

%images

%settings for Xiaoqing's eye

[centers,radii] = imfindcircles(gray_image,[50 60],'ObjectPolarity','dark', ...

'Sensitivity',0.97,'EdgeThreshold',0.03);%can also use bright

%delete(h) % Delete previously drawn circles

% %settings for Maigh's eye

% [centers,radii] = imfindcircles(gray_image,[60 70],'ObjectPolarity','dark', ...

% 'Sensitivity',0.983,'EdgeThreshold',0.07);%can also use bright

% %delete(h) % Delete previously drawn circles

%%%%%%%%%%%%%%%%%%%%%%%%%%%%%%%%%%%%%%%%%%%%%%%%%%%%%%%%%%%%%%%%%%%%%%%%

%Settings for Alex's eye

%%%%%%%%%%%%%%%%%%%%%%%%%%%%%%%%%%%%%%%%%%%%%%%%%%%%%%%%%%%%%%%%%%%%%%%%

```

```
% % % [centers,radii] = imfindcircles(gray_image,[50 60],'ObjectPolarity','dark', ...  
  
% % % 'Sensitivity',0.99,'EdgeThreshold',0.15);%can also use bright  
  
%delete(h) % Delete previously drawn circles  
  
%h = viscircles(centers,radii); %used to view circles on a plot;  
  
%toggled off here due to the magnitude of images and circles  
  
eyepositionarray=cat(1,eyepositionarray, centers);  
  
%adds each obtained circle location information into the  
  
%eyepositionarray  
  
end
```

```
eyepositionarray=eyepositionarray*0.026458333;  
  
%converts complete eye position array from pixels to centimeters  
  
normalizedpositionarray=eyepositionarray(:,1)-eyepositionarray(1);  
  
%normalizes all data to baseline by taking the baseline eye position as  
  
%the origin point for all data
```

```
angularpositionarray=atan((1/screendistance)*normalizedpositionarray);
```

```
%converts position to angle of saccade
```

```
%
```

```
%in sample single saccade stimulus difference is 5.4cm or 204px for
```

```
%reference
```

```
hold on
```

```
plot(linspace(0,v.duration*10^3,length(angularpositionarray)),
```

```
angularpositionarray(:,1),'Color',[0.5,0.5,0.5]);
```

```
plot(linspace(0,v.duration*10^3,length(angularpositionarray)),
```

```
gradient(angularpositionarray(:,1))*10^3,'--r');
```

```
% plots all angle of saccade throughout the duration of the video
```

```
title('Angle of Saccade over the Duration of the Sample Video')
```

```
xlabel('Time in Milliseconds')
```

```
yyaxis left;
```

```
ylabel('Angular Displacement in Degrees')
```

```
yyaxis right;
```

```
ylabel('Angular Velocity in Degrees/Second')
```

%put axis titles

%

%

%%%%%%%%%

%%%%%%%%%

%%%%%%%%%

%%%%%%%%%

SAMPLE OUTPUT PLOTS



Figure 24 Saccade plot from final software setup and preliminary hardware design shown correlated with individual frame iris detection over saccade duration

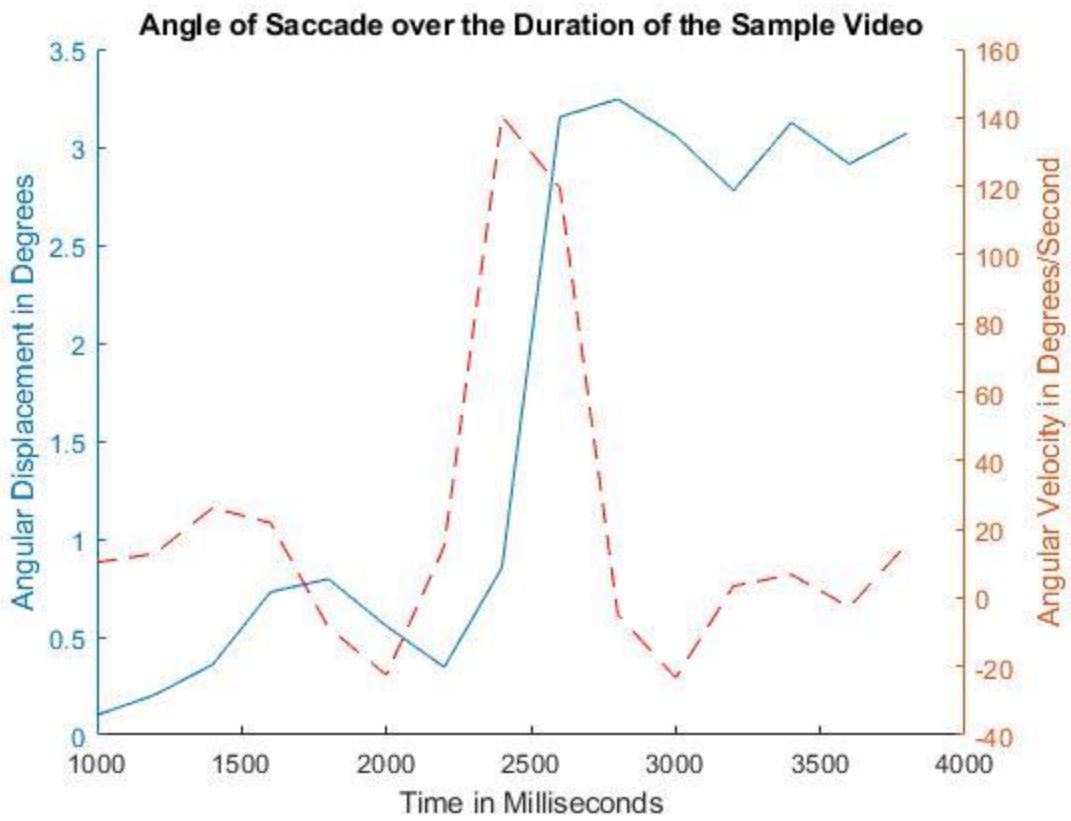


Figure 25 Saccade plot of extracted saccade magnitude and peak velocity over saccade duration in final hardware and software setup

CONCLUSION AND FUTURE WORK

The current experimental iris detection is based on `imfindcircles` which can be converted to C/C++ using the C/C++ Code Generation function of MATLAB Coder. The conversion of `imagesetalyzer` to an Android-based app would increase mobility of the system. The data analysis is currently limited to devices that can run MATLAB to use this built-in function. There are also other software components such as the visual stimulus and background video recorder that could be merged as well into the app. There are some computational concerns as the computing power of a smartphone may not be as strong as that of a desktop computer. However, the modular design lends itself to be used in multiple data transfer chains.

The iris detection may be further automated and refined by a finalized hardware design which would standardize iris radii as well as maintain stable conditions between trials. Another interesting endeavor would be to use binarized images to reduce the computational load of pixel voting.

Another future step would be to test this device in live subjects beyond the healthy subjects tested in this project. This would require an IRB proposal and approval to proceed. However, the device must be tested on the target populations to ensure robust accuracy. A key population would be to implement the system on athletes in high-contact sports who have higher risks for concussions.

Overall, the data is accurate to experimental data obtained on higher-end experimental set-ups. The peak velocity and saccade magnitude linearity is shown, for example, on the data obtained by this system. The theoretical mathematics of saccade parameters are still maintained

in a device that costs significantly less than current measures, is mobile, and requires little to no training to use.

This device has many further steps before it can be implemented in the widespread target populations. However, this project has provided a proof-of-concept for a smartphone-based device that may be able to diagnose neurological dysfunctions using a machine-learning approach to iris detection leading to improved saccade analysis.

ACKNOWLEDGEMENTS:

The author would like to thank Dr. Patrick Kumavor for reviewing and guiding this project as well as serving as a mentor for other research endeavors as well as Alexandra Liberti for contributing to hardware and software analysis.

REFERENCES:

- [1] J. A. Aarli *et al*, "NEUROLOGICAL DISORDERS: Public health challenges," World Health Organization, Switzerland, 2006.
- [2] T. J. Atherton and D. J. Kerbyson, "Size invariant circle detection," *Image Vision Comput.*, vol. 17, (11), pp. 795-803, 1999.
- [3] S. Bal, "Incidence and Prevalence of Major Neurologic Disorders," *US Pharm*, vol. 43, (1), pp. 24, 2018.
- [4] D. H. Ballard, "Generalizing the Hough transform to detect arbitrary shapes," *Pattern Recognit*, vol. 13, (2), pp. 111-122, 1981.
- [5] S. Cannon, "The Neurology of Eye Movements (Contemporary Neurology Series)," *Arch. Ophthalmol.*, vol. 110, (3), pp. 326-326, 1992.
- [6] E. R. Davies, *Machine Vision: Theory, Algorithms, Practicalities*. 2004.
- [7] A. Dogra and P. Bhalla, "Image sharpening by gaussian and butterworth high pass filter," *Biomedical and Pharmacology Journal*, vol. 7, (2), pp. 707-713, 2014.

- [8] J. D. Enderle and W. Zhou, "Models of Horizontal Eye Movements, Part I: A 3rd Order Linear Saccade Model," *Synthesis Lectures on Quantum Computing*, vol. 5, (1), pp. 1-159, 2010.
- [9] C. L. Gooch, E. Pracht and A. R. Borenstein, "The burden of neurological disease in the United States: A summary report and call to action," *Ann. Neurol.*, vol. 81, (4), pp. 479-484, 2017. . DOI: 10.1002/ana.24897 [doi].
- [10] R. Hsu, M. Abdel-Mottaleb and A. K. Jain, "Face detection in color images," *IEEE Trans. Pattern Anal. Mach. Intell.*, vol. 24, (5), pp. 696-706, 2002.
- [11] R. T. Kumar, S. K. Raja and A. Ramakrishnan, "Eye detection using color cues and projection functions," in *Proceedings. International Conference on Image Processing*, 2002, .
- [12] R. J. Leigh and D. S. Zee, "The neurology of eye movements," in Anonymous 2015, .
- [13] S. Lohr, "Facial Recognition Is Accurate, if You're a White Guy," *The New York Times*, [<https://www.nytimes.com/2018/02/09/technology/facial-recognition-race-artificial-intelligence.html>]. 2018.
- [14] M. Maschke *et al*, "Incidence and prevalence of neurological disorders associated with HIV since the introduction of highly active antiretroviral therapy (HAART)," *J. Neurol. Neurosurg. Psychiatry.*, vol. 69, (3), pp. 376-380, 2000.
- [15] (2019). *imfindcircles Find circles using circular Hough transform* . Available: <https://www.mathworks.com/help/images/ref/imfindcircles.html>.

[16] (2 November 2018). *Neurological Disease* [neurological disorders].

Available: <https://medlineplus.gov/neurologicdiseases.html>.

[17] S. Moghal *et al*, "Prevalence of movement disorders in elderly community residents," *Neuroepidemiology*, vol. 13, (4), pp. 175-178, 1994. . DOI: 10.1159/000110376 [doi].

[18] R. S. Moser and P. Schatz, "Enduring effects of concussion in youth athletes," *Archives of Clinical Neuropsychology*, vol. 17, (1), pp. 91-100, 2002.

[19] (). *Neurological Diagnostic Tests and Procedures Fact Sheet* [neurological disorders].

Available: <https://www.ninds.nih.gov/Disorders/Patient-Caregiver-Education/Fact-Sheets/Neurological-Diagnostic-Tests-and-Procedures-Fact>.

[20] A. Ng, "Introduction to Machine Learning," vol. Stanford University for Coursera, 2019.

[21] J. O'Brien *et al*, "Role of radiology in geriatric care: a primer for family physicians," *Can. Fam. Physician*, vol. 55, (1), pp. 32-37, 2009. . DOI: 55/1/32 [pii].

[22] E. Over *et al*, "Coarse-to-fine eye movement strategy in visual search," *Vision Res.*, vol. 47, (17), pp. 2272-2280, 2007.

[23] S. J. K. Pedersen, "Circular hough transform," *Aalborg University, Vision, Graphics, and Interactive Systems*, vol. 123, (6), 2007.

[24] D. Purves, "Neuroscience 2nd Edition. Sunderland (MA) Sinauer Associates. 2001," .

[25] S. Razdan *et al*, "Prevalence and pattern of major neurological disorders in rural Kashmir (India) in 1986," *Neuroepidemiology*, vol. 13, (3), pp. 113-119, 1994. . DOI: 10.1159/000110368 [doi].

[26] U. Samadani, "A new tool for monitoring brain function: eye tracking goes beyond assessing attention to measuring central nervous system physiology," *Neural Regen. Res.*, vol. 10, (8), pp. 1231-1233, 2015. . DOI: 10.4103/1673-5374.162752 [doi].

[27] K. A. Scopaz and J. R. Hatzenbuehler, "Risk modifiers for concussion and prolonged recovery," *Sports Health.*, vol. 5, (6), pp. 537-541, 2013. . DOI: 10.1177/1941738112473059 [doi].

[28] A. H. Snijders *et al*, "Neurological gait disorders in elderly people: clinical approach and classification," *The Lancet Neurology*, vol. 6, (1), pp. 63-74, 2007.

[29] P. Termsarasab *et al*, "The diagnostic value of saccades in movement disorder patients: a practical guide and review," *J. Clin. Mov. Disord.*, vol. 2, pp. 14-015-0025-4. eCollection 2015, 2015. . DOI: 10.1186/s40734-015-0025-4 [doi].

[30] K. Toennies, F. Behrens and M. Aurnhammer, "Feasibility of hough-transform-based iris localisation for real-time-application," in *Object Recognition Supported by User Interaction for Service Robots*, 2002, .

[31] (2019). *Neurological Disorders* [neurological disorders].

Available: https://www.ucsfhealth.org/conditions/neurological_disorders/.

[32] (). *Methods of measuring eye movements.*

Available: <https://www.liverpool.ac.uk/~pcknox/teaching/Eymovs/emeth.htm>.

[33] (). *The parameters of eye movement.*

Available: <https://www.liverpool.ac.uk/~pcknox/teaching/Eymovs/params.htm>.

[34] P. Yalinay Dikmen, E. Ilgaz Aydinlar and G. Karlikaya, "Expected and Experienced Pain Levels in Electromyography," *Noro Psikiyatr Ars*, vol. 50, (4), pp. 364-367, 2013. . DOI: 10.4274/npa.y6699 [doi].

[35] H. Yuen *et al*, "Comparative study of Hough transform methods for circle finding," *Image Vision Comput.*, vol. 8, (1), pp. 71-77, 1990.

[36] R. Zemblys, "Eye-movement event detection meets machine learning," *Biomedical Engineering 2016*, vol. 20, (1), 2016.

[37] Z. Zhu, K. Fujimura and Q. Ji, "Real-time eye detection and tracking under various light conditions," in *Proceedings of the 2002 Symposium on Eye Tracking Research & Applications*, 2002, .

APPENDIX:

CODE FOR SUPPLEMENTARY SOFTWARE:

FRAME EXTRACTOR

EYETEST2FRAMES

```
%%%%%%%%%%%%%%%%%%%%%%%%%%%%%%%%%%%%%%%%%%%%%%%%%%%%%%%%%%%%%%%%%%%%%%%%
%%%%%%%%%%%%%%%%%%%%%%%%%%%%%%%%%%%%%%%%%%%%%%%%%%%%%%%%%%%%%%%%%%%%%%%%
%%%%%%%%%%%%%%%%%%%%%%%%%%%%%%%%%%%%%%%%%%%%%%%%%%%%%%%%%%%%%%%%%%%%%%%%
%%%%%%%%%%%%%%%%%%%%%%%%%%%%%%%%%%%%%%%%%%%%%%%%%%%%%%%%%%%%%%%%%%%%%%%%
%%%%%%%%%%%%%%%%%%%%%%%%%%%%%%%%%%%%%%%%%%%%%%%%%%%%%%%%%%%%%%%%%%%%%%%%

clear

clc

global outputFolder v

path = fullfile(uigetdir);

% extracts user-specified directory %

movieFullFileName = fullfile(path, uigetfile);

% extracts user-specified file from user-specified directory %

v = VideoReader(movieFullFileName)
```

```

% intakes video from file %

D=v.Duration*v.FrameRate

% determines the number of frames based on the length of the video and the frame rate%

[path, baseFileName, extentions] = fileparts(movieFullFileName);

path = pwd;

outputFolder = sprintf('%s/Movie Frames from %s', path, baseFileName);

%makes file from the movie to store the frames in%

if ~exist(outputFolder, 'dir')

    mkdir(outputFolder);

end

for k = 1:D

%extracts each frame and saves it with specified syntax%

    this_frame = readFrame(v);

outputBaseFileName = sprintf('Frame %4.4d.jpg', k);

outputFullFileName = fullfile(outputFolder, outputBaseFileName);

    imwrite(this_frame, outputFullFileName, 'jpg')

end

```

%%

%%

%%

%%

%%

%%

CODE FOR ALTERNATIVE DESIGNS

BINARIZED IMAGE APPROACH

```
%figure()
```

```
eye= imread('Frame 0033.jpg');
```

```
%imshow(eye);
```

```
%medfilteye=medfilt2(grayeye);
```

```
global bineye bineye3
```

```
grayeye = rgb2gray(eye);
```

```
level = graythresh (grayeye);
```

```

bineye= imbinarize(grayeye, level);

bineyesize = size(bineye);

col = round(bineyesize(2)/2)-90;

row = min(find(bineye(:,col)));

boundary = bwtraceboundary(bineye,[row, col], 'N');

%another round of bineye

bineye2= imbinarize(grayeye, 0.2);

bineyesize2 = size(bineye2);

col2 = round(bineyesize2(2)/2)-90;

row2 = min(find(bineye2(:,col2)));

boundary2 = bwtraceboundary(bineye2,[row2, col2], 'N');

bineye3=imbinarize(grayeye, 0.15);

%To test

%medfilt2 , stdev, nhood with ppt images

%also pass it through binimage

figure()

```

```
subplot(2,2,1);

imshow(eye);

title('Original Image');

subplot(2,2,2)

imshow(grayeye);

title('Grayscale Image');

subplot(2,2,3);

imshow(bineye);

title(['Bin level is ', num2str(level), ' based on Otsu method']);

subplot(2,2,4);

imshow(bineye)

hold on;

plot(boundary(:,2),boundary(:,1),'g','LineWidth',3);

title('Boundaries detected and traced');

figure()

subplot(2,1,1)

imshow(bineye2)
```

```
hold on;  
  
plot(boundary2(:,2),boundary2(:,1),'r','LineWidth',3);  
  
title('Boundary traces with lower binary level 0.4');  
  
subplot(2,1,2)  
  
imshow(bineye3);  
  
title('Binarized with even lower level of 0.15');
```

IMAGE FILTERING

HIGH PASS FILTER

```
filename=uigetfile('*.jpg','Select image file');

RGB=imread(filename);

I=rgb2gray(RGB);

k=fspecial('log',[5 5],2.0); %Laplacian of gaussian filter kernel. Try different numbers for best
results

k2=fspecial('unsharp'); %Kernel for making edges more pronounced

%k3=fspecial('average'); %Lowpass (averaging) filter kernel

%I_LPF=imfilter(I,k3); %Low pass filter using averaging

I_LPF=imgaussfilt(I,6.0);% Gaussian lowpass filter. Play with the different parameters

I_HLPF=I-I_LPF; % convert lowpass to highpass

I_HPF_Lap=imfilter(I,k); %First order high pass filter

I_HPF_Sp=imfilter(I,k2);

% I_HPF2=imfilter(I_HPF,k2); %Second order high pass filter

imagesc(I_HPF_Lap);

title('Laplacian of gaussian high pass filter');
```

```
colorbar
```

```
figure;
```

```
imagesc(I_HPF_Sp);
```

```
title('High pass filter (sharp)');
```

```
colorbar
```

```
figure;
```

```
imagesc(I_HLPF);
```

```
title('Gaussian high pass filter');
```

```
colorbar
```

OTHER FILTER SYSTEMS

```
global i
```

```
filename=uigetfile('*.jpg','Select image file');
```

```
RGB=imread(filename);
```

```
I=rgb2gray(RGB);
```

```
nhood=3;
```

```
imagesc(I);
```

```
colorbar
```

```
title('Original Image');
```

```
;
```

```
IEF=entropyfilt(I,true(nhood));
```

```
imagesc(IEF);
```

```
colorbar
```

```
title('Entropy');
```

```
figure
```

```
Isdf=stdfilt(IEF,true(nhood));
```

```
imagesc(Isdf);
```

```
colorbar
```

```
title('Standard Deviation of Entropy');
```

```
figure
```

```
Isdf=stdfilt(I,true(nhood));
```

```
imagesc(Isdf);
```

```
colorbar
```

```
title('Standard Deviation');
```

DOT MATRIX

```
clc
```

```
clear
```

```
xy = [1:24]*1000;
```

```
[X, Y] = meshgrid(xy);
```

```
xyo = xy([4 11]);
```

```
figure(1)
```

```
plot(X, Y, 'k')
```

```
axis square
```